

Proceedings of The Canadian Society for Mechanical Engineering International Congress 2018
CSME International Congress 2018
May 27-30, 2018, Toronto, On, Canada

Application of FBG optical sensors to in-situ monitoring the thermo-mechanical behaviour of cold spray coated samples

Bahareh Marzbanrad, Farid Ahmed, Hamid Jahed, Ehsan Toyserkani
MME Department, University of Waterloo
Waterloo, Canada

Abstract— In this research, a fiber Bragg grating (FBG) sensor is employed for monitoring thermal and mechanical strain induced by severe plastic deformation during high thermal and mechanical strain rate of cold spray technique. The FBG sensors are embedded in magnesium alloy substrates and the strain evolutions of the substrates are recorded during the cold gas spray coating process. In these experiments, the localized transient thermo-mechanical strain induced in the close vicinity of the substrate surface is monitored. Qualitative analysis of the complicated spectra shapes obtained during coating and cooling processes demonstrates the repeatability and sensitivity of the sensors in this condition. In addition, the obtained result from FBG sensors reveals the existence of compressive strain in the substrate near the interface during peening; however, it is released after a few second because of the high impact temperature of cold spray coating.

Keywords- *FBG Sensor; Cold Gas Spray; Magnesium alloy*

I. Introduction

The FBG sensors have been employed for sensing the different stimulus such as strain, temperature, pressure, and vibration, because of the unique advantages (small size, immunity to external interferences, ability to operate in harsh environmental conditions, etc.) over other commercial sensors. The optical measurement is safe and superior over electrical one for wide range of applications in harsh environments such as lightening, high electromagnetic fields and in temperature ranging from cryogenic environments to high temperatures of up to 1000°C [1-3]. FBG is typically constructed by writing periodic index modulation in the core of an optical fiber, which may later be coated with acrylate, polyimide, or organic modulated ceramic for specific application [4]. The grating works as an invisible reflector that reflects only certain wavelengths of light [5]. Deformation of a grating device in presence of external stimulus is represented by wavelength shifts, which can be recorded by an interrogator. If the deformation across the grating part is not uniform (e.g. localized loading), the reflected wavelength shape appears to be asymmetric. Such asymmetric behavior of FBG spectrum can be analyzed to quantify the thermal/mechanical strains. With the recent advancement in optical data acquisition systems, FBG sensors are able to record data (the wavelength changes) with high frequency. Hence, the FBG sensors are

ideal candidates for the measurement of localized high temperature and high strain rate; a new application for FBG sensor that needs to be addressed.

Cold gas spray is a method of coating in which, high velocity particles impact a surface and create a layer of solid-state coating [6, 7]. Adiabatic shear deformation of the particles upon impact generates the localized heat and shear deformation at the contact area of the powder and substrate, which leads to mechanical and/or metallurgical bonding. Based on the cold spray mechanism, thermal softening and work hardening are in competition; since 90% of impact kinetic energy is dissipated as a heat in less than 100 ns, thermal softening may occur rather than work hardening [8]. Although the cold spray should be a low temperature coating method, the generated heat during impact process may cause to relieve the beneficial residual stress due to peening process and microstructural changes, which needs to be considered. However, it may depend on coating and substrate material characteristics. This is a special localized high temperature and fast deformation phenomenon that can be observed in situ by using a FBG sensor.

In this study, we investigate the capability of FBG sensor for revealing the localized residual stress development in magnesium during the cold spray coating process. A FBG with grating length of 4 mm was embedded in the magnesium sample; however, the phenomena happen over a few hundred microns below the substrate surface. Therefore, only a small part of the FBG was under stress. The goal of this research is to study the dynamic deformation of the substrate as well as temperature changes simultaneously. They determine the equilibrium situation of the magnesium grains, which may cause compressive or tensile residual stress and localized heat effects such as stress relief.

A. Response of FBG sensor to the localized external stimulus

During the experiments, any mechanical and/or thermal strain changes can shift the reflected wavelengths of the FBG sensors, which can be recorded by an interrogator. In this research, Sm125-200 with one optical channel, and the wavelength accuracy of 10 pm was employed.

The relationship between the wavelength shifts, strain, and temperature changes is specified according to the following equations:

$$\varepsilon = \frac{1}{K} \left(\frac{\Delta\lambda}{\lambda_0} - \alpha_\delta \times \Delta T \right) \quad (1)$$

$$\varepsilon = \varepsilon_m + \varepsilon_T \quad (2)$$

$$\varepsilon_T = \alpha_{sp} \times \Delta T \quad (3)$$

$$\alpha_\delta = \frac{\delta n/n}{\delta T} \quad (4)$$

where, $\Delta\lambda$ is the wavelength shift, λ_0 is the base wavelength at test start, k is the gauge factor, ε is the total strain caused by force (ε_m) and temperature (ε_T), α_δ is defined by the change of the refractive index with temperature, α_{sp} is the expansion coefficient of the sample (1°K), and ΔT is the temperature change ($^\circ\text{K}$). For measuring temperature, a type K thermocouple (300 μm wires) was attached to each sample; hence, it would be able to detect the temperature of substrate surface during coating process. The FBG was used to record the strain developed in the sample. However, if the FBG sensor experiences a non-uniform strain over the grating length, the response of the sensor will be different. For instance, if only a part of the grating experiences the strain while the rest remains unresponsive to the phenomenon, the spectral response comes only from the sensor length that is exposed to the strain. In this case, the sensor works as two individual in-line FBGs with different grating periods. Based on the optomechanical model proposed by Alemohammad *et al.* [9], the spectra of the FBG sensor was simulated when distributed strain was applied over the grating length of FBG sensor. The optomechanical model was employed to illustrate the response of the FBGs to localized strain. For instance, it was assumed that an external stimulus applied tensile strains of 0.001 and 0.002 over 200 μm length of the 10 mm grating (Fig 1). Based on the simulation, the main wavelength peak of the sensor before applying the strain was a single peak with high intensity (black spectrum) (Fig 1-b). However, the induced strain created a lopsided peak at the right side of the main peak, while the intensity of the original peak was decreased. Increasing the strain from 0.001 to 0.002 led to significant lopsided peak shifts compared to the previous case. Therefore, it is predicted that in case of the localized strain on a small part of the grating, the main spectrum will be split to lopsided peaks and the position of the peaks is proportional to strain amplitude.

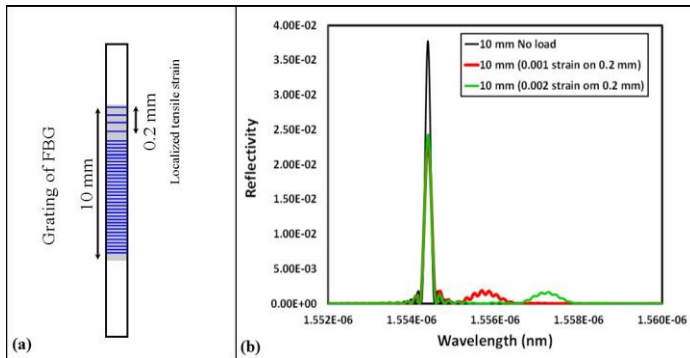


Fig 1: a) A schematic of grating part of FBG sensor under localized tensile loading; b) the spectra obtained from optomechanical model in different strain amplitudes

II. Experimental Procedure

In this study, three AZ31B-H24 Mg alloy samples with 4mm thickness were used for in-situ strain and temperature measurement. Properties of the Mg alloy can be found in [10]. The shape of samples is shown in Fig 2-a. For these tests, the specimens were finely polished to minimize surface roughness.

A. Sample preparation

An initial step in developing a smart Mg alloy structure is specimen layout in a way that it would be enabled to accommodate the FBG sensors, respecting to the location of sensing the strain and temperature in the sample during the cold spray tests. Since the maximum strains are induced around 100 μm below the substrate surface due to peening process, the grating needs to be embedded very close to the surface for optimum outcome. For this, two different embedding positions of the optical sensors were considered so that the propagation axis of the fiber makes an angle of 90° or 45° with the substrate surface. Three different holes were drilled in the samples. Two holes with a diameter of 700 μm was drilled at the angle of 90° and 45° relative to the substrate surface for embedding the FBGs, while the 1mm hole was drilled in the sample for embedding the thermocouple. Fig 2-a shows the positions of thermocouple and FBG sensors in the samples. After drilling the holes, all the samples were heat treated in order to relieve the induced stress during manufacturing and preparation of the samples. The heat treatment process was conducted at a temperature of under 260°C (500°F) for 15 minutes, followed by air-cooling [11].

B. Preparation of the FBG sensors

In this work, 10 mm long FBG sensors inscribed in Corning SMF-28 optical fiber with initial center wavelengths of 1540 nm and 1560 nm were utilized (Fig 2-b). To have more precise results, the polyimide jacket was removed from the grating part of the FBG sensors before embedding inside the magnesium alloy sample's holes.

Then, the bare FBG sensors were accommodated in such a way that the 4mm length of grating was placed inside the holes and the rest was out of the sample. High temperature EPO-TEK 353ND adhesive was used for embedding the sensors and thermocouple. To cure the epoxy resin, the samples were heated at 150°C for an hour using an electric furnace. Fig 2-c shows the setup of the sample with embedded sensors and thermocouple. After embedding the sensors and curing the resin, the 6mm extra part of the grating were cut and gently polished with 800-grit sandpaper.

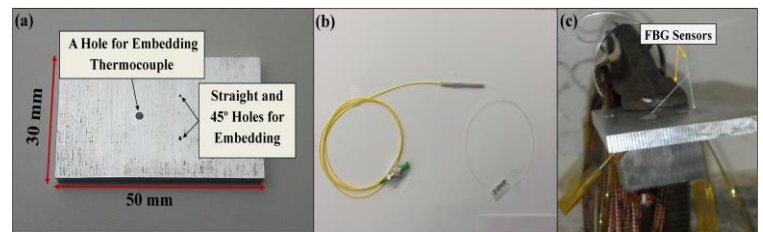


Fig 2: a) AZ31B-H24magnesium alloy sample; b) Corning SMF-28 FBG sensor; c) Test sample setup of embedding the sensor with thermal epoxy

Fig 3-a illustrates the reflected spectrum of one of the sensors, which demonstrates the initial center wavelength of 1560 nm before embedding the sensor. After embedding, the shape of spectrum was completely rough-and-tumble and the peak broadening was also observed (Fig 3-b). Moreover, the intensity of the peak was changed after curing process. Fig 3-c shows the spectrum changes after cutting and polishing the extra part of the sensor. As seen, the spectrum became narrower after cutting in comparison to the same sensor after embedding.

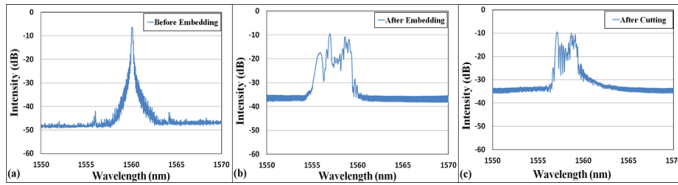


Fig 3: FBG spectrum, a) before embedding; b) after embedding with thermal epoxy; c) after cutting and polishing the sensor

C. Cold spray process

A commercial Cold Spray system (SST Series P) manufactured by Centerline was used to deposit spherical commercial Al7075 powder (supplied by Centerline) with the mean particle size of 23 μ m (measured by Retsch technology, Camsizer XT) on the smart magnesium alloy samples. The chemical compositions of Al7075 powders are listed in Table 1. Al7075 powders were accelerated through the De Laval UltiLife™ Nozzle with reciprocating movement on the samples. To create a coating layer of aluminium with 300 μ m thickness, low porosity and high hardness, the Nitrogen gas was used with stagnation pressures of 200 Psi and temperatures of 400°C to produce the suitable particles velocity. For more clarification, all requirement parameters for conducting the relatively high quality of coating by cold spray deposition are listed in Table 2.

Table 1: Chemical compositions of Al7075 coating powders

Composition	Aluminum (Al)	Zinc (Zn)	Iron (Fe)	Nickel (Ni)	Chromium (Cr)	Copper (Cu)	Magnesium (Mg)	Other Elements
Weight %	90	5.20	0.35	0.005	0.25	1.55	2.35	0.30

Table 2: Cold Spray Coating Parameters [12]

Flow Gas	Nitrogen
Gas Temperature	400 °C
Gas Pressure	200 Psi (1.4 MPa)
Powder Feed Rate	8 gr/min (5 rpm)
Nozzle Speed	2 mm/s
Step Over	1.2 mm
Stand-off Distance	12 mm
Nozzle Type	De Laval <u>UltiLife</u> ™
Nozzle Length	120 mm
Nozzle Orifice	2 mm
Nozzle Exit Diameter	6.3 mm

III. Results and discussions

In-situ monitoring of mechanical and thermal strain was implemented during the cold spray coating process through embedded FBG sensors in Mg alloy substrates. Response of FBG sensors to axial deformation (extension or contraction of the gratings) due to thermal and/or mechanical stimulus is a linear wavelength change; an increase in grating period due to elongation of the fiber causes a red shift (higher wavelength) of the central wavelength and vice versa [13, 14]. Fig 4 shows a set of critical spectrums obtained at different nozzle positions during cold spraying for three different embedded samples. It should be noted that during the cold spray experiments, only the responses of sensors embedded at a 45° directions were recorded. In all of the tests as shown in Fig 4-a, the first curves reveal the response of the sensors after embedding (before running the cold spray tests). When the nozzle approached the sensors, peak broadening and spectral red shift were observed (Fig 4-b). In this condition, thermal strain due to the carrier gas temperature leads to the shifting and broadening of the spectrums. The asymmetric spectra of the sensors were generated because of the non-uniform strains induced along the grating length. The spectra were expanded towards higher wavelengths, which emphasized on elastic strains accumulation close to the substrate surface. With decreasing the distance between nozzle and sensors, more stretching and shifting of spectrums expected. However, with placing the nozzle exactly above the sensors, in spite of higher predicted temperature due to the adiabatic shear instability for particles/substrate bonding, the peaks narrowing were observed while the main peaks still showed more transition to the right (Fig 4-c). This shape change of spectrum uncovers that a significant compressive residual stress is developed in the surface and as a consequence, a compressive strain is induced by peening and severe plastic deformation during the deposition, diminishing the effect of thermal expansion. This observation clarified the contrast between the peening effect and temperature deviation. After passing the nozzle the peaks became broaden and shifted even further to the right where the sign of compressive strains was no more observable. This indicates that the induced stress weakened in the substrate in a few second. Fig 4-e shows the shape of the spectrums after the cold spray tests were completed and the Mg alloy samples reached to the room temperature. The shapes of spectrums became narrow; however, the peaks were shifted to the right compare to the very initial spectrums (Fig 4-a). For Test #2 before recording the spectrum after cold spray at room temperature, the FBG failed; hence, the spectrum was not recorded. It should be noted that during the experiments the temperature of samples were recorded by thermocouples, simultaneously. The results obtained from the thermocouples showed that the substrates' temperature was increased up to 330°C [15], while the annealing temperature of magnesium alloy AZ31B is about 260°C that confirmed the results obtained from FBG sensors, which demonstrated the relieving stress. Fig 5 shows the magnesium alloy sample embedded with two FBG sensors and thermocouple after conducting the cold spray coating tests.

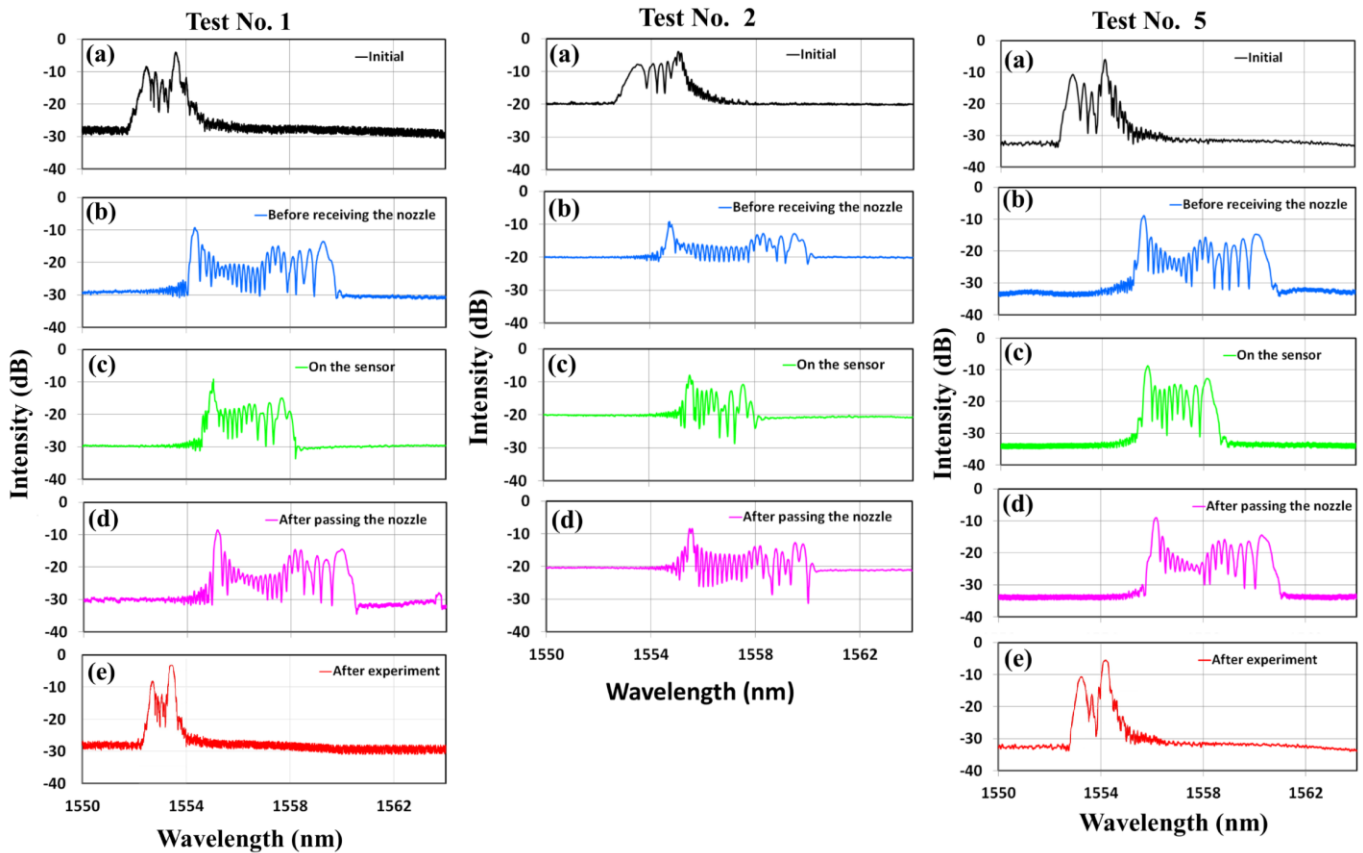


Fig 4: The spectrums of FBG sensors for three different tests in five different situations: a) after embedding a sensor; b) during coating at 10mm distance from the nozzle; c) coating on the sensor; d) at 10 mm after passing the nozzle; e) after coating at RT.

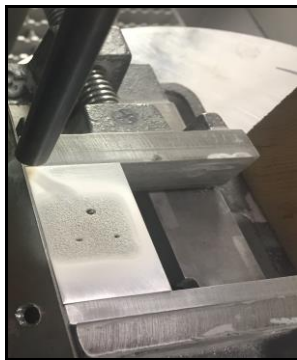


Fig 5: Smart magnesium alloy tested sample after cold spray coating test

For more clarification, the bandwidths and shifts of spectrums at different locations were measured: 1) before conducting the cold spray tests; 2) before receiving the nozzle to the tip of the sensor location; 3) where the nozzle was on the tip of sensors; 4) after passing the nozzle; and, 5) after the cold spray tests were completed and the part arrived at room temperature. The bar graphs in Fig 6-a depict the changes of spectrum bandwidth during the experiments. Usually, the bandwidth of the reflection peak is defined by Full-Width-Half-

Maximum (FWHM), which is the width of 50% of the main peak. In addition, the averages of the widths for all experiments in each situation were added to the bar graphs. Based on the measurements, for all experiments when the nozzle was on top of the sensor the bandwidths of spectra were decreased, significantly, while before and after receiving the nozzle during the cold spray the bandwidths were increased due to the raise in temperature.

In addition, the wavelength shifts during the experiments and after the cold spray tests at room temperature were measured (see Fig 6-b). Based on the observations, the wavelengths shifted to the right noticeably, during the experiments because of increased temperature; however, subtle shifts occurred at different situations during the tests. After conducting the cold spray tests, a significant amount of wavelengths shifts observed in all samples (yellow bars in Fig 6-b), which indicates the existence of tensile strains. These results highlight the effect of temperature due to carrier gas and adiabatic shear deformation on the evolution of tensile strains in the coated samples. It is noticeable that the stress relief process releases the residual elastic energy of the material while in these cases, not only the compressive stresses due to peening process were relieved, but also tensile residual strains were imposed in the substrates. This can be explained by

considering the thermal mismatch strain of the Al7075 coating and AZ31B-H24 substrate, which created tensile residual strain during the cooling process (after coating).

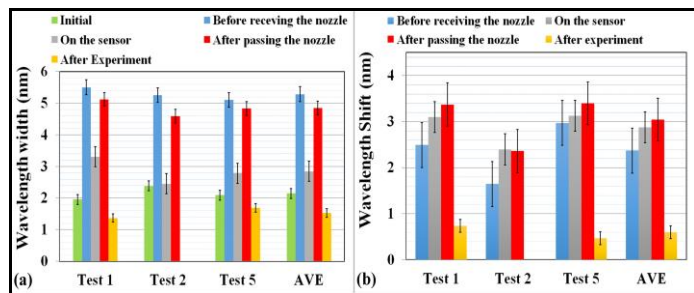


Fig 6: a) Wavelength width for different situations in three tests;
b) Wavelength shifts for different situations in three tests

IV. Conclusion

In this research, the capability of FBG sensors for detecting the localized thermal and mechanical strain induced in cold spray coated magnesium alloy is investigated. Localized increase in temperature and distributed deformation in a small area below the surface was implemented through the cold spray coating process. To this end, the FBG sensors were embedded in a magnesium alloy substrates and responses of the sensor recorded during the coating process. This observation revealed that the FBG sensor is able to tolerate the thermal and mechanical impact of the cold spray coating and detect the high mechanical and thermal strain rate during the process. In addition these experiments demonstrated that a compressive residual stress was induced in the substrate during coating, but it was relieved after a few second, which could be an evidence for stress relief of the magnesium alloy substrate due to the coating temperature.

V. References

[1] M. Fokin, Underlying mechanisms, applications, and limitations of chemical composition gratings in silica based fibers, *Journal of Non-Crystalline Solids* 349 (2004) 98-104.
 [2] V.P. Wnuk, Mendez, S. Ferguson, T. Graver, Process for mounting and packaging of Fiber Bragg Grating strain sensors for use in harsh environment application, *Smart structures conference, SPIE, 2005*, pp. 5758-6.
 [3] J.-H. Ha, P. Muralidharan, D.K. Kim, Hydrothermal synthesis and characterization of self-assembled h-WO₃ nanowires/nanorods using EDTA salts, *Journal of Alloys and Compounds* (2009) 446-451.
 [4] M.M. Werneck, R.C.S.B. Allil, B.A. Ribeiro, F.V.B.d. Nazaré, *A Guide to Fiber Bragg Grating Sensors, InTech2013*.
 [5] E. Udd, W.B. Spillman, *Fiber Optic Sensors: An Introduction to Engineer and Scientists*, 2nd ed., Wiley2011.
 [6] A. Papyrin, V. Kosarev, S. Klinkov, A. Alkhimov, V. Fomin, *Cold Spray Technology*, 1st ed., Elsevier, Amsterdam, 2006.
 [7] G. Shayegan, H. Mahmoudi, R. Ghelichi, J. Villafuerte, J. Wang, M. Guagliano, H. Jahed, Residual stress induced by cold spray coating of magnesium AZ31B extrusion, *Materials & Design* 60 (2014) 72-84.

[8] H. Assadi, H. Kreye, F. Gärtner, T. Klassen, Cold spraying – A materials perspective, *Acta Mater.* 116 (2016) 382-407.
 [9] H. Alemohammad, E. Toyserkani, Modeling and Analysis of Fiber Optic Bragg Grating Shape Sensors, *ASME International Mechanical Engineering Congress and Exposition, Proceedings of IMECE2007, Seattle, Washington, USA, 2007*.
 [10] S.B. Behraves, H. Jahed, S. Lambert, Characterization of magnesium spot welds under tensile and cyclic loadings, *Materials & Design* 32(10) (2011) 4890-4900.
 [11] *ASM Handbook*, ASM International1991.
 [12] S. Dayani, R. Ghelichi, S. Shaha, J. Wang, H. Jahed, The impact of Al7075 cold spray coating on the fatigue life of AZ31B cast alloy, *Surface and Coatings Technology* 337 (2018) 150-158
 [13] B. Marzbanrad, H. Jahed, E. Toyserkani, On the sensitivity and repeatability of fiber Bragg grating sensors used in strain and material degradation measurement of Magnesium alloys under cyclic loads, *Int. J. Adv. Manufact. Technol.* 86(9-12) (2016) 3453-3461.
 [14] R. Kashyap, *Fiber Bragg Gratings, Second Edition ed., Elsevier, United States of America, 2010*.
 [15] B. Marzbanrad, H. Jahed, E. Toyserkani, On the evolution of substrate's residual stress during cold spray process: A parametric study, *Materials & Design* 138 (2018) 90-102.